Velocity Profile Sampling In Large Stack & Flare Gas Piping

By
Eric Harman
CEESI

Acknowledgements:
I would like to thank Dr. Aaron Johnson at NIST, Gaithersburg, MD. Dr. Johnson contributed an enormous amount of work to this project. NIST requires internal peer review for papers written by NIST employees. At the time of publication, the peer review process could not be completed. My sincere gratitude goes out to my colleague and friend.

Abstract:
Large stacks and flare gas lines are commonly measured using path-averaging technologies (ultrasonic meters) and discrete point-averaging meters (averaging pitot tubes). These flow meters are calibrated and verified insitu using pitot traverse sampling. Theoretical velocity profiles are numerically integrated and compared to Centroid-of-equal-areas, Chebyshev, and Gauss Legendre Quadrature averaging techniques. The number of sampling points, sampling methodology, and uncertainty analyses are plotted against Reynolds number dependent power-law profiles. Swirling and skewed velocity profiles are also included in the analyses.

Executive Summary:
Centroid-of-equal-areas, Chebyshev, and Gauss Legendre Quadrature averaging techniques were examined and compared at different Reynolds numbers in fully-developed, swirling, and skewed velocity profiles. Chebyshev and Gauss Legendre Quadrature showed significant improvement over Centroid-of-equal-areas in fully developed profiles. Uncertainties given in Table 2 show the "hidden" errors associated with discrete velocity sampling for the given profiles typically seen in stack and flare gas lines.

Background:
Measuring stack and flare gas flow rates can be extremely challenging. Large flow turndowns (maximum velocity to minimum velocity), varying gas composition, changes in density, and distorted velocity profiles all contribute to making stack and flare gas measurement difficult. Additionally:

- These applications usually require a low pressure drop across the measuring device which excludes orifice plates, cone meters and most other full-throated devices.
- It is difficult and expensive to duplicate large stack and flare gas pipe runs at test laboratories.
- Offshore flare lines have limited straight lengths of piping which produce skewed, swirling flows.
- Stacks are usually preceded by upstream profile-distorting elbows, tees, and fittings.
- The most common flow meters used to measure stack and flare gas lines are ultrasonic meters (path-averaging), and averaging pitot tubes (sample-averaging meters). These technologies can be influenced by distorted velocity profiles.

Of the challenges listed above, this paper focuses on the errors resulting from changing velocity profiles due to increasing Reynolds number, and profile distortions caused by upstream piping disturbances.

Velocity Profiles:

As the velocity increases in a pipe, the shape of the velocity profile changes from a parabolic (pointed) contour to a blunt (flatter) contour. This changing contour can be characterized by the pipe's Reynolds number and was first studied by Reynolds, Prandtl, Nikuradse and others [(1)]. Empirical formulas were developed to describe the velocity profile as a function of the pipe's radius. One such equation is called the Power Law:

$$\frac{u}{U_0} = \left(1 - \frac{r}{R}\right)^{\frac{1}{N}}$$

Where:

$u = Local\ velocity$
$U_0 = Lenterline\ velocity$
$r = Distance\ from\ the\ center\ to\ the\ point\ in\ question$
$R = Pipe\ radius$
$N = Power\ Law\ exponent\ (a\ function\ of\ pipe\ Reynolds\ Number)$

More complicated equations have been developed to characterize the contour of a velocity profile with increasing Reynolds number. Some of these equations better characterize the steep velocity gradient as the fluid approaches the pipe wall. Pipe surface roughness and turbulence levels can also influence the shape of the velocity profile. Two such equations are the Bogue-Metzner equation[(2)], and the Gilmont equation[(3)]. While these equations better describe velocity profiles as the fluid approaches the wall, they offer little improvement over the Power Law in the core velocity region where bulk flow rates are predominately determined. Furthermore, the Bogue-Metzner does not have a closed form integratable solution. For these reasons this paper uses the Power Law to describe velocity profiles.

Fully Developed and Distorted Velocity Profiles

The figure below shows three typical velocity profiles: a fully developed flow profile, an axial-symmetric distorted profile resulting from swirling flow, and an asymmetric skewed velocity profile.

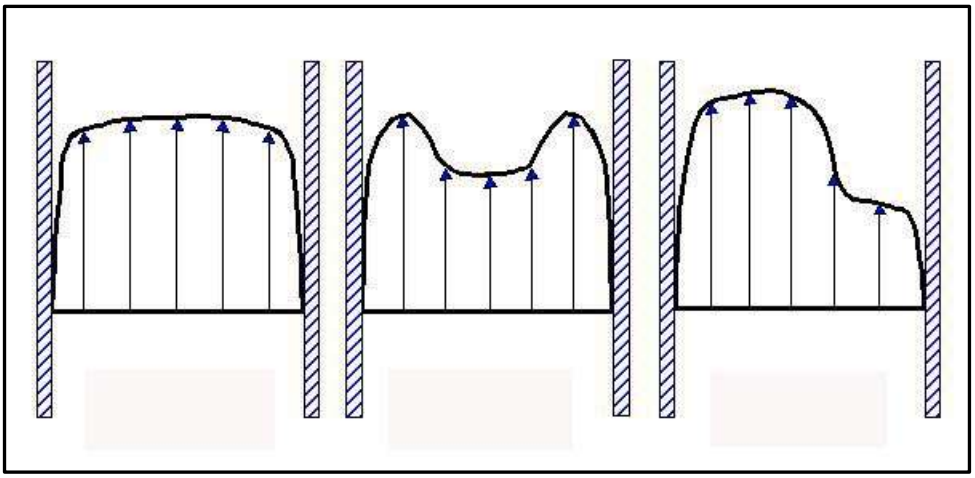

Figure 1.
Three Typical Velocity Profiles
(From Left To Right, Fully Developed, Swirling Flow, Skewed Flow)

Discussion of Swirling Flow:

Swirling flow is characterized by fluid velocity vectors traveling radially or in a non-axial direction. The user is usually only interested in the axial component of flow because only the axial component contributes to the flow rate traveling down the pipe. Non-axial fluid vectors can have a profound effect on the performance of a flow meter or a sampling pitot tube. If the effect is known, corrections can be made to a meter's flow coefficient to compensate for the swirl angle. Most pitot tubes can be rotated in the flow stream to detect the magnitude of swirl. Many pitot tubes are tested in wind tunnels or laboratories at different swirl angles so that the effect of swirl can be accounted for. This allows the user to determine the axial velocity component. Paper assumes pitot tube sampling has already been adjusted for the swirl angle. A careful distinction should be made: Velocity profiles described in this paper are limited to the velocity vectors in the axial direction and do not include any radial, or non-axial components.

Insitu Pitot Traverse Calibration:

Because of the inability to duplicate pipe runs in laboratories, stack and flare meters are usually calibrated or verified insitu by performing a pitot traverse. A pitot tube is inserted into the flow stream at specific locations; discrete velocities are measured and then averaged to determine the overall flow rate in the pipe. A pitot traverse usually is performed in two axes. In large pipes or in lines that have short lengths of upstream and downstream piping more traversing axes are utilized. The United States EPA has published guidelines covering the minimum number of traversing axes and the minimum number of sampling locations, see 40-CFR Part 60, found at www.epa.gov. EPA guidelines use a sampling methodology called Centroid-of Equal-Areas. Figure 2 shows a circular pipe being divided into multiple area increments. Figure 3 shows a typical pitot traversing mechanism.

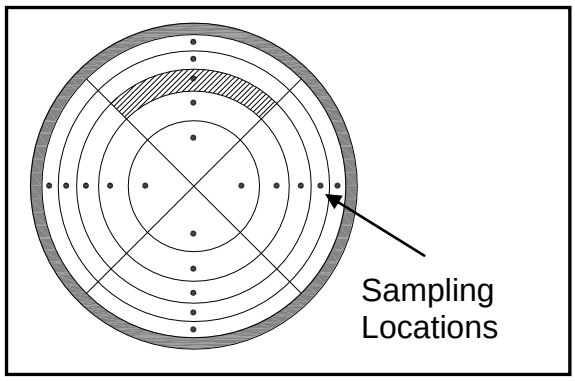

Figure 2.

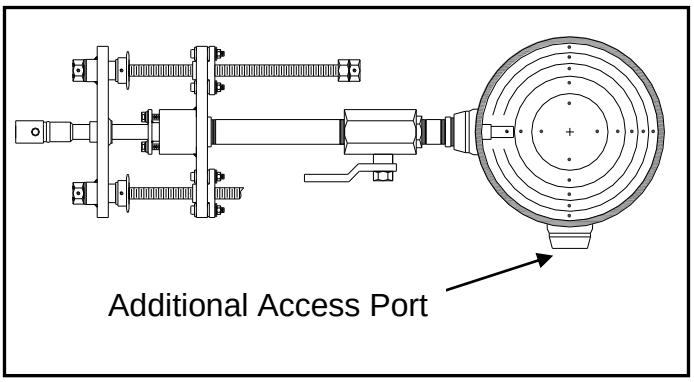

Figure 3.

Hidden Errors In Pitot Traverse Sampling

It is often assumed that pitot traversing uncertainty is only a function of the user's ability to measure the pipe diameter, the uncertainty of the pitot tube's flow coefficient, and the instruments used to measure the differential pressure, temperature, pressure, and gas composition. Unfortunately there is a hidden error that is often overlooked or ignored. This hidden uncertainty is how well the sampling locations characterize the velocity profile. Three averaging techniques are considered in the following analyses: Centroid-of-equal-areas, Chebyshev, and Gauss Legendre Quadrature.

When Conducting A Pitot Traverse Several Questions Arise:

1. How many sampling points should be taken?
2. Will adding more sampling points improve the uncertainty?
3. How many axes should be traversed?
4. As the velocity in the pipe changes will the uncertainty of the pitot traverse be affected?
5. How will flow disturbances affect my pitot traverse?

Test Cases Chosen For Analysis:

Pipe Size

A 48" schedule standard pipe was chosen for analysis because in 2012, NIST & CEESI will be performing pitot traverse testing in a 48" pipe. Results from this paper's numerical integration and averaging methodologies will be compared to experimental data.

Gas Velocities

Flare gas lines can operate from 0.3 mps to 120 mps (during upset conditions). Stacks in power plants commonly operate between 6-45 mps. To cover this wide range of velocities the following five velocities were chosen for comparative analysis: 0.6, 6.1, 18.3, 42.7, 91.4 mps.

Temperature, Static Pressure, Specific Gravity, & Gas Composition:

Temperature, static pressure, specific gravity, gas composition, and other fluid parameters can have a large impact on a pitot traverse and the resulting flow rate calculation. These variables can be measured independently and corrected for separately. Because the theoretical results in this paper will be tested at NIST & CEESI in air, the following conditions were chosen:

Fluid: Air
Static Pressure: 1 Atmosphere (14.696 psia)
Temperature: 15.5°C (60°F)

Sampling Methods:

Centroid-of-equal-areas, Chebyshev, and Gauss Legendre Quadrature

Number Of Sampling Locations And Number Of Traversing Axes:

For a 48" pipe with at least 8 pipe diameters upstream and 2 pipe diameters downstream United States EPA document 40-CFR Part 60 recommends 12 sampling points per traversing axis and two axes. To understand how the number of sampling points affects the resulting uncertainty, 8 sampling points and 16 sampling points were also chosen.

Velocity Profiles

1. Power Law*
2. Simulated swirling flow (polynomial function)
3. Simulated skewed flow (polynomial function)

Method Of Analysis:

Numerical methods were applied by integrating the velocity functions. Skewed velocity profiles were analyzed using two traversing axes 90° apart, and combining their resulting errors. Excel spreadsheets were used to tabulate data found in Table 2.

*Power Law Exponents were based on curve fitting experimental data in Table 5.3 in Fundamentals of Pipe Flow[1]. The resulting curve fit is shown in Chart 1 on the following page.

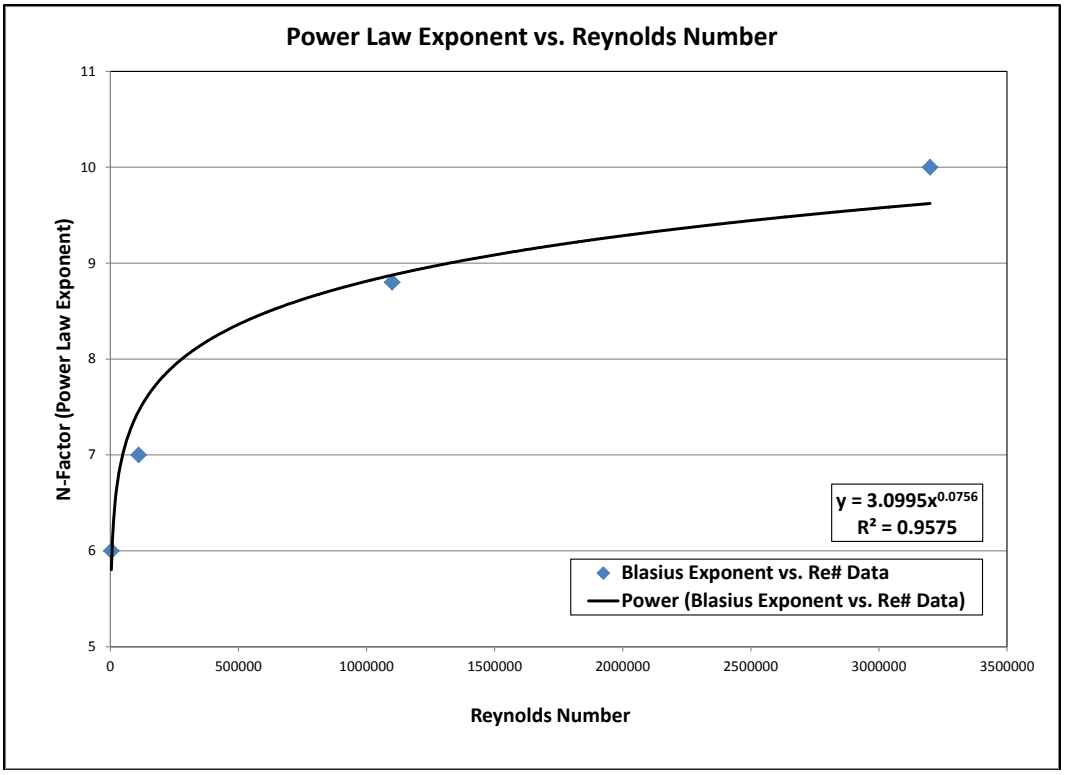

Chart 1
Power Law Exponent 'N' vs. Reynolds Number [1]

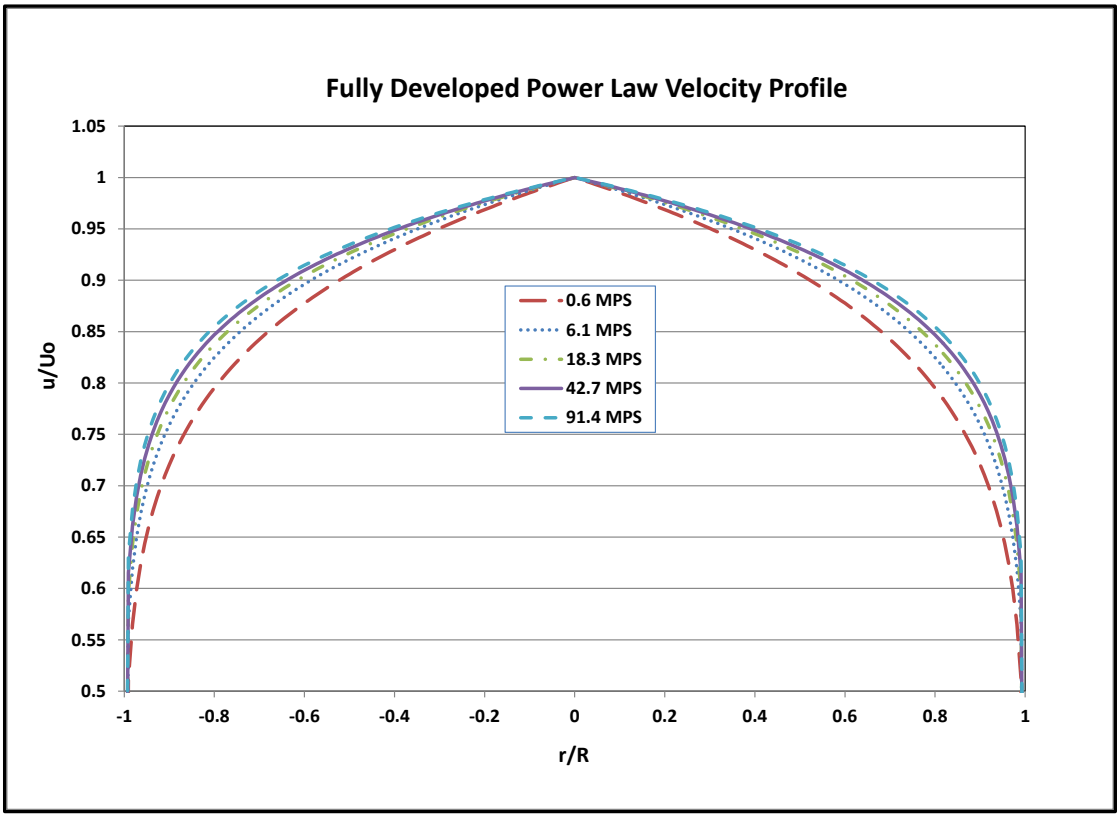

Chart 2
Power Law Profiles

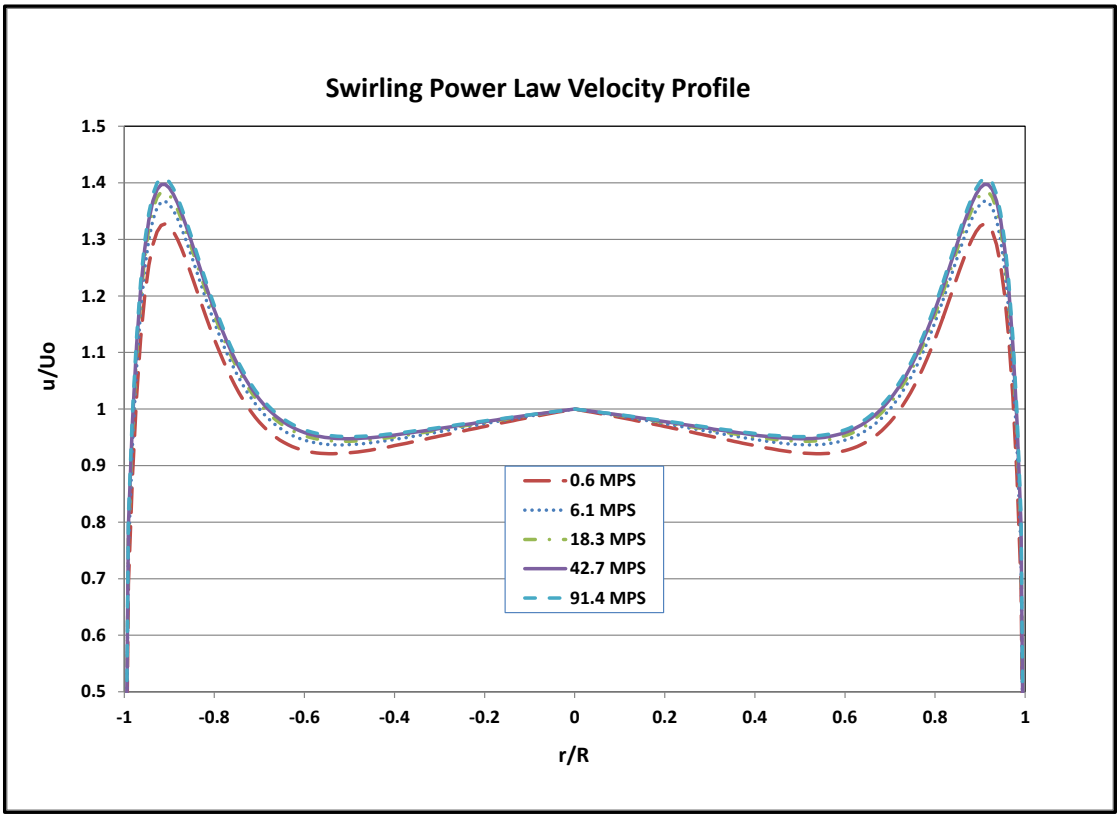

Chart 3
Distorted (Axial-Symmetric) Swirling Flow

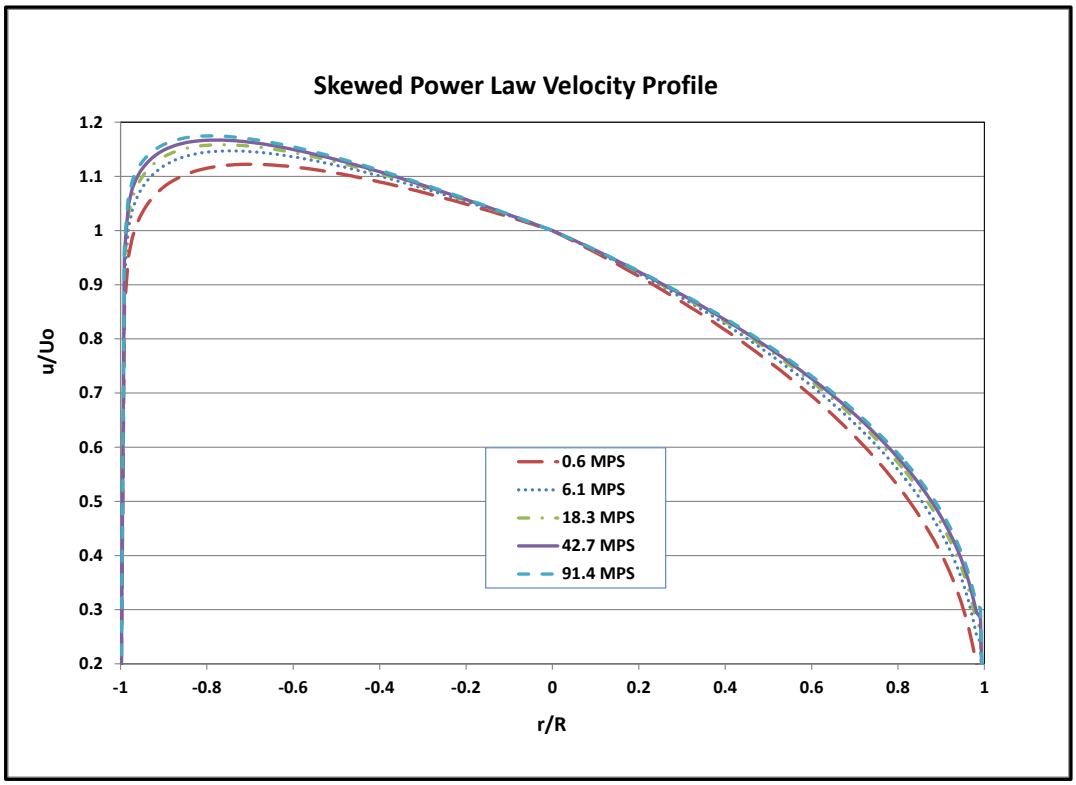

Chart 4
Distorted (Asymmetric) Skewed Flow

Centroid of Equal Areas Locations
Radius Ratios

20 Point	18 Point	16 Point	14 Point	12 Point	10 Point	8 Point	6 Point	4 Point
-0.9747	-0.9718	-0.9682	-0.9636	-0.9574	-0.9487	-0.9354	-0.9129	-0.8660
-0.9220	-0.9129	-0.9014	-0.8864	-0.8660	-0.8367	-0.7906	-0.7071	-0.5000
-0.8660	-0.8498	-0.8292	-0.8018	-0.7638	-0.7071	-0.6124	-0.4082	0.5000
-0.8062	-0.7817	-0.7500	-0.7071	-0.6455	-0.5477	-0.3536	0.4082	0.8660
-0.7416	-0.7071	-0.6614	-0.5976	-0.5000	-0.3162	0.3536	0.7071	
-0.6708	-0.6236	-0.5590	-0.4629	-0.2887	0.3162	0.6124	0.9129	
-0.5916	-0.5270	-0.4330	-0.2673	0.2887	0.5477	0.7906		
-0.5000	-0.4082	-0.2500	0.2673	0.5000	0.7071	0.9354		
-0.3873	-0.2357	0.2500	0.4629	0.6455	0.8367			
-0.2236	0.2357	0.4330	0.5976	0.7638	0.9487			
0.2236	0.4082	0.5590	0.7071	0.8660				
0.3873	0.5270	0.6614	0.8018	0.9574				
0.5000	0.6236	0.7500	0.8864					
0.5916	0.7071	0.8292	0.9636					
0.6708	0.7817	0.9014						
0.7416	0.8498	0.9682						
0.8062	0.9129							
0.8660	0.9718							
0.9220								
0.9747								

Chebyshev Locations
Radius Ratios

20 Point	18 Point	16 Point	14 Point	12 Point	10 Point	8 Point	6 Point	4 Point
-0.9788	-0.9776	-0.9740	-0.9705	-0.9660	-0.9572	-0.9473	-0.9239	-0.8881
-0.9185	-0.8947	-0.8924	-0.8745	-0.8434	-0.8290	-0.7699	-0.7071	-0.4597
-0.8660	-0.8743	-0.8388	-0.8136	-0.7958	-0.7071	-0.6382	-0.3827	0.4597
-0.8102	-0.7642	-0.7425	-0.7071	-0.6057	-0.5592	-0.3203	0.3827	0.8881
-0.7361	-0.7071	-0.6698	-0.5814	-0.5373	-0.2891	0.3203	0.7071	
-0.6768	-0.6450	-0.5444	-0.4849	-0.2586	0.2891	0.6382	0.9239	
-0.5862	-0.4854	-0.4513	-0.2410	0.2586	0.5592	0.7699		
-0.5000	-0.4466	-0.2266	0.2410	0.5373	0.7071	0.9473		
-0.3954	-0.2103	0.2266	0.4849	0.6057	0.8290			
-0.2046	0.2103	0.4513	0.5814	0.7958	0.9572			
0.2046	0.4466	0.5444	0.7071	0.8434				
0.3954	0.4854	0.6698	0.8136	0.9660				
0.5000	0.6450	0.7425	0.8745					
0.5862	0.7071	0.8388	0.9705					
0.6768	0.7642	0.8924						
0.7361	0.8743	0.9740						
0.8102	0.8947							
0.866	0.9776							
0.9185								
0.9788								

Table 1
Centroid-of-Equal Areas & Chebyshev Sampling Locations

Equal Area Sample Method
8 Sampling points

Profile Shape	Velocity (MPS)	% Error
Developed	0.6	0.68
Developed	6.1	0.62
Developed	18.3	0.59
Developed	42.7	0.57
Developed	91.4	0.55
	Average Error=	0.60
Swirled	0.6	2.80
Swirled	6.1	2.70
Swirled	18.3	2.66
Swirled	42.7	2.63
Swirled	91.4	2.60
	Average Error=	2.68
Skewed	0.6	-0.53
Skewed	6.1	-0.55
Skewed	18.3	-0.56
Skewed	42.7	-0.58
Skewed	91.4	-0.59
	Average Error=	-0.56

Equal Area Sample Method
12 Sampling points

Profile Shape	Velocity (MPS)	% Error
Developed	0.6	0.44
Developed	6.1	0.41
Developed	18.3	0.39
Developed	42.7	0.38
Developed	91.4	0.36
	Average Error=	0.40
Swirled	0.6	1.48
Swirled	6.1	1.43
Swirled	18.3	1.40
Swirled	42.7	1.38
Swirled	91.4	1.36
	Average Error=	1.41
Skewed	0.6	-0.82
Skewed	6.1	-0.82
Skewed	18.3	-0.82
Skewed	42.7	-0.82
Skewed	91.4	-0.83
	Average Error=	-0.82

Equal Area Sample Method
16 Sampling points

Profile Shape	Velocity (MPS)	% Error
Developed	0.6	0.33
Developed	6.1	0.30
Developed	18.3	0.29
Developed	42.7	0.28
Developed	91.4	0.27
	Average Error=	0.29
Swirled	0.6	0.92
Swirled	6.1	0.89
Swirled	18.3	0.87
Swirled	42.7	0.86
Swirled	91.4	0.85
	Average Error=	0.88
Skewed	0.6	-0.96
Skewed	6.1	-0.95
Skewed	18.3	-0.94
Skewed	42.7	-0.94
Skewed	91.4	-0.94
	Average Error=	-0.95

Chebyshev Sample Method
8 Sampling points

Profile Shape	Velocity (MPS)	% Error
Developed	0.6	0.36
Developed	6.1	0.34
Developed	18.3	0.32
Developed	42.7	0.31
Developed	91.4	0.30
	Average Error=	0.33
Swirled	0.6	1.05
Swirled	6.1	1.02
Swirled	18.3	1.00
Swirled	42.7	0.98
Swirled	91.4	0.97
	Average Error=	1.00
Skewed	0.6	-0.93
Skewed	6.1	-0.92
Skewed	18.3	-0.91
Skewed	42.7	-0.91
Skewed	91.4	-0.91
	Average Error=	-0.92

Chebyshev Sample Method
12 Sampling points

Profile Shape	Velocity (MPS)	% Error
Developed	0.6	0.22
Developed	6.1	0.20
Developed	18.3	0.20
Developed	42.7	0.19
Developed	91.4	0.18
	Average Error=	0.20
Swirled	0.6	0.20
Swirled	6.1	0.19
Swirled	18.3	0.19
Swirled	42.7	0.18
Swirled	91.4	0.18
	Average Error=	0.19
Skewed	0.6	-1.10
Skewed	6.1	-1.07
Skewed	18.3	-1.06
Skewed	42.7	-1.06
Skewed	91.4	-1.05
	Average Error=	-1.07

Chebyshev Sample Method
16 Sampling points

Profile Shape	Velocity (MPS)	% Error
Developed	0.6	0.17
Developed	6.1	0.16
Developed	18.3	0.15
Developed	42.7	0.15
Developed	91.4	0.14
	Average Error=	0.16
Swirled	0.6	0.16
Swirled	6.1	0.15
Swirled	18.3	0.14
Swirled	42.7	0.14
Swirled	91.4	0.14
	Average Error=	0.14
Skewed	0.6	-1.15
Skewed	6.1	-1.12
Skewed	18.3	-1.11
Skewed	42.7	-1.10
Skewed	91.4	-1.09
	Average Error=	-1.11

Gaussian Sample Method
8 Sampling points

Profile Shape	Velocity (MPS)	% Error
Developed	0.6	0.23
Developed	6.1	0.21
Developed	18.3	0.20
Developed	42.7	0.20
Developed	91.4	0.19
	Average Error=	0.21
Swirled	0.6	0.22
Swirled	6.1	0.21
Swirled	18.3	0.20
Swirled	42.7	0.19
Swirled	91.4	0.19
	Average Error=	0.20
Skewed	0.6	-1.08
Skewed	6.1	-1.06
Skewed	18.3	-1.05
Skewed	42.7	-1.05
Skewed	91.4	-1.04
	Average Error=	-1.06

Gaussian Sample Method
12 Sampling points

Profile Shape	Velocity (MPS)	% Error
Developed	0.6	0.10
Developed	6.1	0.09
Developed	18.3	0.09
Developed	42.7	0.09
Developed	91.4	0.09
	Average Error=	0.09
Swirled	0.6	0.08
Swirled	6.1	0.07
Swirled	18.3	0.07
Swirled	42.7	0.07
Swirled	91.4	0.07
	Average Error=	0.07
Skewed	0.6	-1.22
Skewed	6.1	-1.19
Skewed	18.3	-1.18
Skewed	42.7	-1.17
Skewed	91.4	-1.16
	Average Error=	-1.18

Gaussian Sample Method
16 Sampling points

Profile Shape	Velocity (MPS)	% Error
Developed	0.6	0.05
Developed	6.1	0.05
Developed	18.3	0.05
Developed	42.7	0.05
Developed	91.4	0.05
	Average Error=	0.05
Swirled	0.6	0.04
Swirled	6.1	0.04
Swirled	18.3	0.04
Swirled	42.7	0.04
Swirled	91.4	0.04
	Average Error=	0.04
Skewed	0.6	-1.27
Skewed	6.1	-1.23
Skewed	18.3	-1.22
Skewed	42.7	-1.21
Skewed	91.4	-1.20
	Average Error=	-1.23

Table 2
Uncertainty of Centroid-of-Equal Areas, Chebyshev, and Gauss Legendre Quadrature

Discussion Of Results:

From Table 2, the following observations can be made:

1. Decreasing the velocity from 91.4 to 0.6 mps only increases the uncertainty approximately 0.1%. Discrete velocity sampling is relatively immune to increases in velocity.
2. For fully-developed velocity profiles Chebyshev and Gauss Legendre Quadrature have approximately half the uncertainty as Centroid-of-Equal Areas.
3. For fully-developed velocity profiles increasing the number of sampling points reduces the uncertainty.
4. For distorted velocity profiles increasing the number of sampling points does not always reduce the uncertainty.

References:

1. Benedict, R.P., Fundamentals of Pipe Flow, pp. 178-227, 1980.
2. "Velocity Profiles in Turbulent Pipe Flow", D.C. Bogue & A.B. Metzner. University of Delaware, Newark, Del.
3. "Velocity Profile of Turbulent Flow in Smooth Circular Pipes", R. Gilmont. Reprinted from Measurement & Control, June 1996.
4. Miller, R.W, Flow Measurement Engineering Handbook, Third edition, pp. 5.37-5.40., 1996.
5. American Gas Association: AGA Report No. 9, *Measurement of Gas by Multipath Ultrasonic Meters*, June 1998.
6. ASME Research Committee on Fluid Meters, Fluid Meters, 6th edition, pp. 109-110, 1971.
7. ASME PTC 19.5-2004, Section 9, "Flow Measurement by Velocity Traverse", pp. 97-137, 2004.

Appendix –A-

Math Functions & Integration

$$\frac{u_1(r,\theta)}{U_0} = \left(1 - \frac{r}{R}\right)^{1/n}$$

$$\frac{U_{avg,1}}{U_0} = \frac{Q_1}{\pi R^2 U_0} = \frac{2n^2}{(n+1)(2n+1)}$$

$$\frac{u_2(r,\theta)}{U_0} = \varepsilon_2 \left(\frac{r}{R}\right)\left(1 - \frac{r}{R}\right)^{1/m}\left[A - B\cos^2(q\theta)\right]$$

$$\frac{U_{avg,2}}{U_0} = \frac{Q_2}{\pi R^2 U_0} = \varepsilon_2 \left[\frac{m + 2m^2}{(m+1)(2m+1)(3m+1)}\right]\left[\pi(2A - B) - \frac{B\sin(4\pi q)}{4q}\right]$$

$$\frac{u_3(r,\theta)}{U_0} = \varepsilon_3 \left(1 - \frac{r}{R}\right)\left[\exp\left(\beta\frac{r}{R}\right) - 1\right]$$

$$\frac{U_{avg,3}}{U_0} = \frac{Q_3}{\pi R^2 U_0} = 2\,\varepsilon_3 \left[\frac{\beta + 2 + \exp(\beta)(\beta - 2)}{\beta^3}\right]$$

$$\frac{u_4(r,\theta)}{U_0} = \varepsilon_4 \left(\frac{r}{R}\right)\left[1 - \left(\frac{r}{R}\right)^s\right]\cos(t\theta)$$

$$\frac{U_{avg,4}}{U_0} = \frac{Q_4}{\pi R^2 U_0} = \varepsilon_4 \left[\frac{s}{3(s+3)}\right]\left[\frac{\sin(2\pi t)}{\pi t}\right]$$

1st Velocity Profile Integration

$$\frac{u_1(r,\theta)}{U_0} = \left(1-\frac{r}{R}\right)^{1/n}$$

$$Q_1 = \int_0^{2\pi}\int_0^R r\,u_2\,dr\,d\theta = \int_0^{2\pi}\int_0^R r U_0\left(1-\frac{r}{R}\right)^{1/n} dr\,d\theta$$

$$Q_2 = 2\pi R^2 U_0 \int_0^{2\pi}\int_0^1 z(1-z)^{1/n}\,dz$$

$$Q_2 = \pi R^2 U_0\left[\frac{2n^2}{(n+1)(2n+1)}\right]$$

$$\frac{U_{avg,1}}{U_0} = \frac{Q_1}{\pi R^2 U_0} = \frac{2n^2}{(n+1)(2n+1)}$$

2nd Velocity Profile Integration

$$\frac{u_2(r,\theta)}{U_0} = \varepsilon_2\left(\frac{r}{R}\right)\left(1-\frac{r}{R}\right)^{1/m}\left[A - B\cos^2(q\theta)\right]$$

$$Q_2 = \int_0^{2\pi}\int_0^R r\,u_2\,dr\,d\theta = \int_0^{2\pi}\int_0^R \varepsilon_2 r U_0\left(\frac{r}{R}\right)\left(1-\frac{r}{R}\right)^{1/m}\left[A - B\cos^2(q\theta)\right]dr\,d\theta$$

$$Q_2 = \varepsilon_2 R^2 U_0 \int_0^{2\pi}\int_0^1 z^2(1-z)^{1/m}\left[A - B\cos^2(q\theta)\right]dz\,d\theta$$

$$Q_2 = \varepsilon_2\, R^2 U_0\left[\int_0^1 z^2(1-z)^{1/m}\,dz\right]\left[\int_0^{2\pi}\left[A - B\cos^2(q\theta)\right]d\theta\right]$$

$$Q_2 = \varepsilon_2\, R^2 U_0\left[\frac{m+2m^2}{(m+1)(2m+1)(3m+1)}\right]\left[\pi(2A-B) - \frac{B\sin(4\pi q)}{4q}\right]$$

$$Q_2 = \varepsilon_2 \pi R^2 U_0\left[\frac{m+2m^2}{(m+1)(2m+1)(3m+1)}\right]\left[(2A-B) - \frac{B\sin(4\pi q)}{4\pi q}\right]$$

$$\frac{U_{avg,2}}{U_0} = \frac{Q_2}{\pi R^2 U_0} = \varepsilon_2\left[\frac{m+2m^2}{(m+1)(2m+1)(3m+1)}\right]\left[(2A-B) - \frac{B\sin(4\pi q)}{4\pi q}\right]$$

3rd Velocity Profile Integration

$$\frac{u_3(r,\theta)}{U_0} = \varepsilon_3\left(1-\frac{r}{R}\right)\left[\exp\left(\beta\frac{r}{R}\right)-1\right]$$

$$Q_3 = \int_0^{2\pi}\int_0^R r u_3 dr d\theta = \int_0^{2\pi}\int_0^R \varepsilon_3 r U_0\left(1-\frac{r}{R}\right)\left[\exp\left(\beta\frac{r}{R}\right)-1\right]dr d\theta$$

$$Q_3 = \int_0^{2\pi}\int_0^R r u_3 dr d\theta = 2\,\varepsilon_3\pi R^2 U_0\int_0^1 z(1-z)\left[\exp(\beta z)-1\right]dz$$

$$Q_3 = 2\,\varepsilon_3\pi R^2 U_0\left[\frac{\beta+2+\exp(\beta)(\beta-2)}{\beta^3}\right]$$

$$\frac{U_{avg,3}}{U_0} = \frac{Q_3}{\pi R^2 U_0} = 2\,\varepsilon_3\left[\frac{\beta+2+\exp(\beta)(\beta-2)}{\beta^3}\right]$$

4th Velocity Profile Integration

$$\frac{u_4(r,\theta)}{U_0} = \varepsilon_4\left(\frac{r}{R}\right)\left[1-\left(\frac{r}{R}\right)^s\right]\cos(t\theta)$$

$$Q_4 = \int_0^{2\pi}\int_0^R r u_4 dr d\theta = \int_0^{2\pi}\int_0^R r U_0\varepsilon_4\left(\frac{r}{R}\right)\left[1-\left(\frac{r}{R}\right)^s\right]\cos(t\theta)dr d\theta$$

$$Q_4 = \varepsilon_4 R^2 U_0\int_0^{2\pi}\int_0^1 z^2\left[1-z^s\right]\cos(t\theta)dz d\theta$$

$$Q_4 = \varepsilon_4 R^2 U_0\left[\int_0^1 z^2\left[1-z^s\right]dz\right]\left[\int_0^{2\pi}\cos(t\theta)d\theta\right]$$

$$Q_4 = \varepsilon_4 R^2 U_0\left[\left(\frac{1}{3}\right)\left(1-\frac{3}{s+3}\right)\right]\left[\frac{\sin(2\pi t)}{t}\right]$$

$$Q_4 = \varepsilon_4 \pi R^2 U_0\left[\frac{s}{3(s+3)}\right]\left[\frac{\sin(2\pi t)}{\pi t}\right]$$

$$\frac{U_{avg,4}}{U_0} = \frac{Q_4}{\pi R^2 U_0} = \varepsilon_4\left[\frac{s}{3(s+3)}\right]\left[\frac{\sin(2\pi t)}{\pi t}\right]$$